Geotechnical Aspects of Underground Construction in Soft Ground, Kastner, Emeriault, Dias, Guilloux (eds)
 ISBN 2-9510416-3-2

Simulation of slurry shield behaviour during excavation

A. Sramoon, M. Sugimoto & N. Mukai
Nagaoka University of Technology, Niigata, Japan

K. Takahashi
Japan Railway Construction Public Corporation, Tokyo, Japan

N. Okamura
Sato Kogyo Co., Ltd., Tokyo, Japan

ABSTRACT: To precisely control the alignments of tunnel and shield, the tunnelling operation affecting the shield behaviour should be clearly clarified. The theoretical shield model had been developed to cope with that problem, taking into account of the ground displacement around the shield. This paper shows the simulation results of the slurry shield behaviour during excavation at the curve by applying the actual shield operational control data and the excavation condition to the proposed model. The model performance is discussed by comparing the calculated shield behaviour with the actual one. As a result, the observed shield behaviour is well simulated by the proposed model. The simulation results show that the copy cutter mainly induces the ground displacement, which is a predominant factor influencing the shield tunnelling performance at the curve.

1 INTRODUCTION

Nowadays, slurry shield is widely adopted to use in urban tunnel construction, since it can be employed in a wide range of soil types under the ground water level. Slurry shield tunnelling work is operated based on the previous construction case records by means of an automatic excavation control system. To precisely control the alignments of tunnel and shield, the shield tunnelling operations affecting the shield behaviour, which is defined as rotation and translation of the shield during excavation, should be clearly clarified.

Authors had proposed the model of the loads acting on the shield in order to simulate the shield behaviour during excavation based on the equilibrium conditions, taking account of the ground displacement around the shield (Sugimoto and Sramoon 2002). The loads acting on the shield are composed of the self-weight of machine, force at the shield tail, force due to the shield jack, force acting at the shield face, and force acting on the shield skin plate. The model had been successfully applied to simulate an EPB shield behaviour in a straight alignment (Sramoon et al. 2002).

In this study, slurry shield was employed at the test site with use of the copy cutter in order to facilitate the shield tunnel excavation at the curve. The shield operational control and the excavation condition were observed to discuss the slurry shield performance during excavation at the curve. The simulation result of shield behaviour is compared with that of the observation to verify performance of the proposed model. Furthermore, the factors affecting the shield behaviour are also examined and discussed through the simulation results.

2 SLURRY SHIELD TUNNELLING TEST SITE

The test site was established at the Hiromachi railway tunnel in order to obtain precise and reliable observed data. At the test site location, the overburden depth was approximately 9.50 m and the ground water level was observed approximately at 2.30 m below the ground surface. The parent and child shields were employed for tunnel diameter enlargement purpose, however, only the child shield was used at the

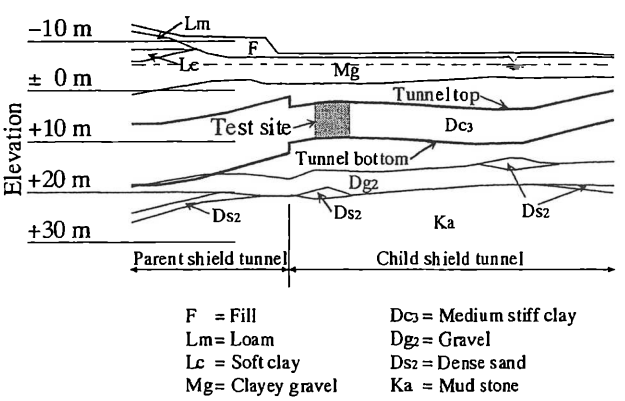

Figure 1. Geological profile at test site location.

test site. The slurry child shield was employed in medium stiff clay throughout the test site with accumulated length of 42 m approximately as shown in Figure 1. The diameter of slurry shield was 7.26 m with 8.415 m in length. After excavation processes, the concrete segment was installed with an outer diameter of 7.10 m and 1.20 m in width. The alignment of tunnel at the test site was the leftward curve with radius of 245 m horizontally. The parent and child shields mechanism and their tunnelling performances for this tunnelling site were well documented by Takahashi & Fukazawa (2001).

The tunnel operation control and the tunnel excavation condition were observed in order to examine their influences on the shield behaviour through the simulation. The observed data were summarized at 20 cm interval, i.e., one segmental ring about six excavation steps, and their characteristics can be described as follows.

2.1 *Tunnel operational control*

The applied jack thrust, jack moments, cutter torque, and copy cutter to control the shield along the planned alignment are shown in Figure 2. Jack thrust F_{3r} was usually applied around 15 MN to mainly encounter against the earth pressure at the face and the friction on the shield skin plate in the shield axis direction as its advance. Since the planned tunnel alignment at the test site is horizontal leftward curve, the horizontal jack moment M_{3p} was usually applied to rotate the shield to the left-hand side to follow the planned alignment, M_{3p} was normally negative in this case. However, sometimes the tunnel alignment did not coincide with the planned alignment, the positive M_{3p} was therefore applied to rotate the shield onto the planned alignment. The vertical jack moment M_{3q} was mainly applied against the vertical moment due to the earth pressure acting on the cutter disc and to maintain the shield on the horizontal plane. The cutter torque CT was generated to rotate the cutter disc against the moment around shield axis due to shearing resistances on the cutter disc and its rotation direction caused the shield rolling around its axis. Therefore, the rotation direction of the cutter disc was alternately changed to maintain the use of equipment inside the shield.

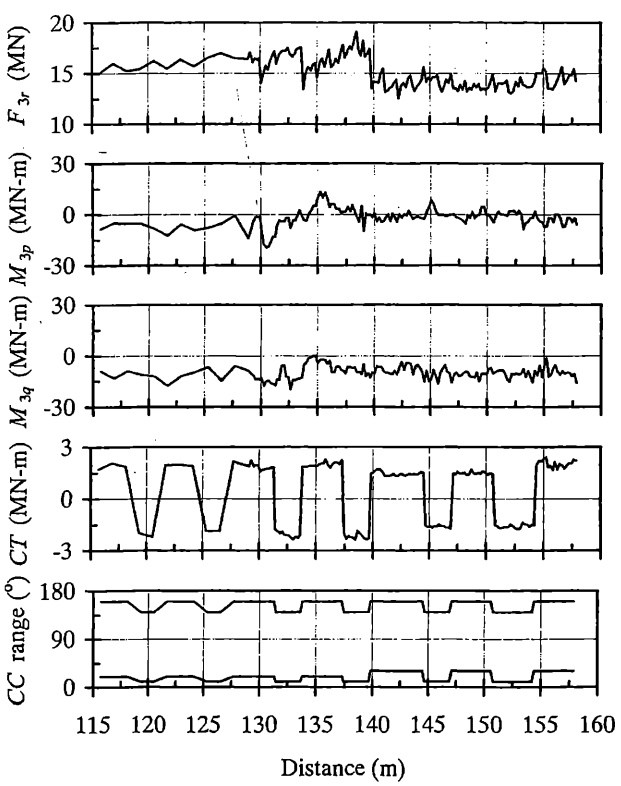

Figure 2. Shield tunnelling operation.

Since the tunnel was excavated at the curve alignment, the copy cutter was employed to increase competence of the excavation at the curve. The copy cutter is done by extruding the steel rod from the edge of cutter disc into the surrounding ground at the specified starting point and remains its length until it reaches the specified closing point by rotating the cutter disc. The copy cutter (CC) range was started from 10° to 160° approximately, measured from the invert of shield in clockwise direction, i.e., at around the left spring line of shield, together with the appropriate M_{3p} in order to rotate the shield towards the left, since the tunnel curve is leftward curve. The length of copy cutter was 7 to 8 cm. Use of the copy cutter increase the excavated area around the cutter disc, which causes reduction of the earth pressure in that area, and make a shield easily translate or rotate to that area.

2.2 *Tunnel excavation condition*

Figure 3 shows excavation conditions for the test site, which is the extending jack stroke between the successive data, excavation time interval, slurry pressure, slurry density, and excavated volume ratio. Since the data was summarised at 20 cm interval, the extending jack stroke is approximately 20 cm. The excavation time interval t_{exc} is approximately 7 minutes for first stage of the test site and then increases up to 20 minutes due to reduction of the jack thrust. t_{exc} was a result of shield velocity v_s. To stabilise the face, the slurry pressure σ_m was applied based on the lateral earth pressure acting at the face of tunnel. In this test site σ_m was applied 150 kPa approximately. The gradient of slurry pressure from the top to bottom of the tunnel face was controlled by the slurry density γ_m. γ_m was used in between 12 to 14 kN/m^3 and it seems correspondent to the jack thrust and excavation time. For perfect excavation, the excavated volume ratio R_v, which is the ratio between calculated excavated volume and removal volume of the

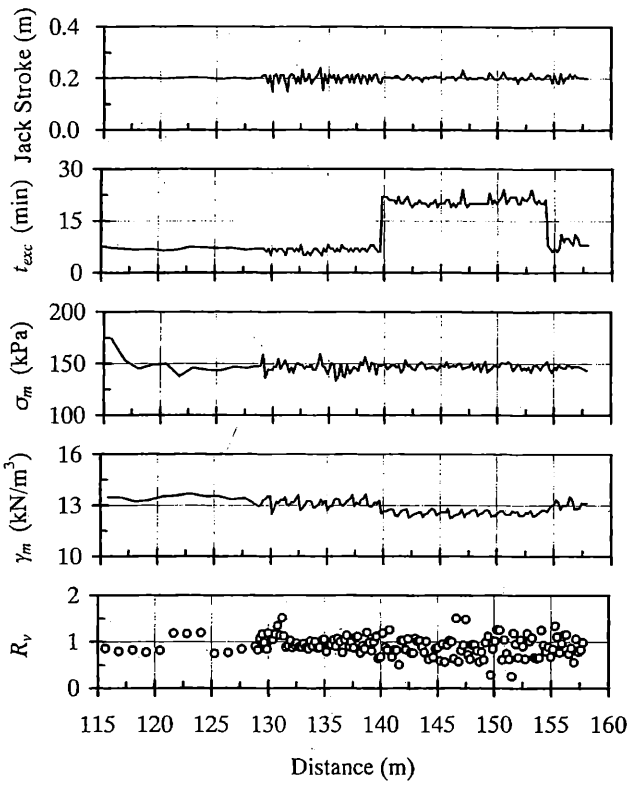

Figure 3. Excavation condition during tunnelling.

excavated ground, should be equal to 1. R_v for this test site indicates that the well excavation control was achieved, since it is close to unity throughout the test.

3 SIMULATION OF SHIELD BEHAVIOUR

The model of the loads acting on the shield during excavation is composed of five forces: force due to the self-weight of machine f_1, force on the shield tail f_2, force due to the jack thrust f_3, force on the cutter disc f_4, and force on the shield periphery f_5, as shown in Figure 4 (Sugimoto & Sramoon 2002). By applying the shield model, the shield behaviour can be obtained based on balance of the forces acting on the shield.

The dimension of tunnel and shield, and the shield jack component are shown in Table 1. Since

Table 1. Dimension of tunnel, machine and ground properties used in the analysis.

Item	Component	Value
Tunnel	Horizontal radius	-245 m
	Vertical radius	∞ m
	Overburden depth	9.50 m
	Groundwater level	2.30 m
	Outer radius of segment	3.55 m
	Width of segment	1.20 m
Shield	Outer radius	3.63 m
	Total length	8.415 m
	Modulus of shield	2.04×10^5 MN/m^2
	Center of erector in C^M	(0.0, 0.0, -3.84) m
	Self-weight	4.686 MN
	Open ratio of cutter face	22.0 %
	Thickness of cutter face	0.705 m
	Radius of chamber	3.58 m
	Length of chamber	1.50 m
	Radius of cutter face	3.64 m
	Cutter disc rotation speed	0.77 rpm
Shield jack	Number of jacks	24
	Cross-sectional area	598.285 cm^2
	Radius of jack	3.34 m
	Length of jack	2.74 m
	Center of jack from cutter face	3.035 m
Ground properties	K_{hmin}, K_{ho}, K_{hmax} [1]	0.614, 0.756, 5.0
	K_{vmin}, K_{vo}, K_{vmax} [1]	0.3, 1.0, 5.0
	k_h, k_v (kN/m^3) [1]	9530, 9530
	Medium stiff clay: c, μ [2]	18.0, 0.0
	Slurry: c, μ [2]	0.0, 0.0

Note: 1. Based on Sugimoto & Sramoon (2002).
2. c is cohesion (kN/m^2) and μ is coefficient of friction.

the shield is excavated entirely in medium stiff clay throughout the test site, the ground properties used in the analysis are also summarized in Table 1. The tunnel operational control shown in Figure 2 and the tunnel excavation condition shown in Figure 3 are also used in the analysis as input parameters. The effective length of over-excavation, which is the difference between the radius of cutter disc and the radius of shield, and the length of copy cutter used in the simulation are 20% and 45% of the actual conditions respectively, since the actual applications may not be fully effective during excavation due to disturbance of ground around the cutter edge. The simulation was started after the whole length of shield lied within the test site and continued to the end of the test site. The significant results of the

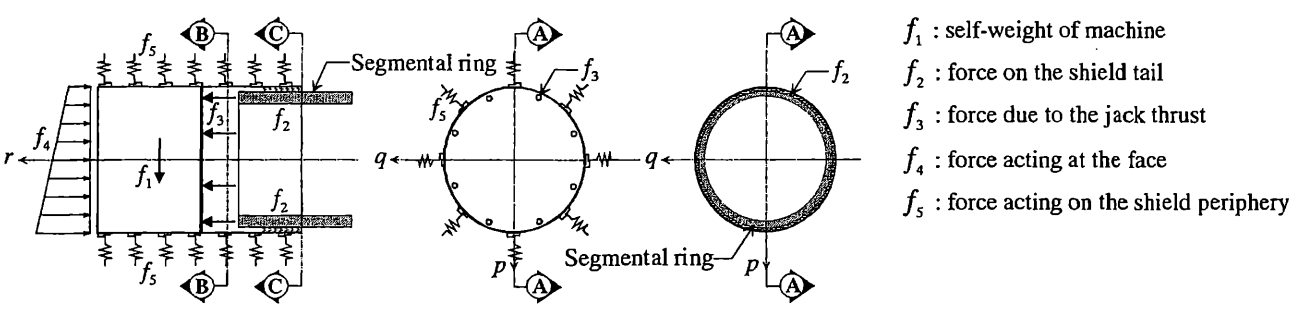

Figure 4. Model of loads acting on shield.

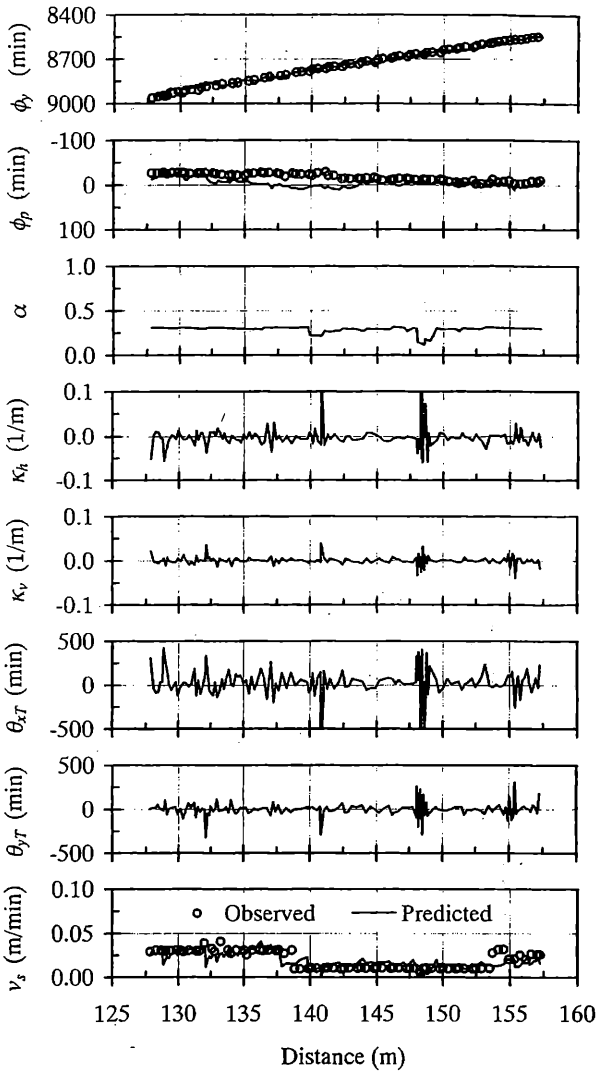

Figure 5. Predicted and observed shield behaviour.

simulation are shown in Figure 5 and can be explained as follows.

The predicted ϕ_y shows a very good agreement with that of the observation, which indicates that the shield rotates towards the left gradually. This is because the shield tries to take the balance for the applied M_{3p} by rotating to the gap, which is generated by the copy cutter. The observed ϕ_p shows that the shield performed look-up throughout excavation at the test site ($\phi_p < 0$). The prediction of ϕ_p shows slight deviation from that of the observation where the applied M_{3q} is close to zero, however, at the other steps the prediction of ϕ_p is in agreement with the observation. Since the change of ϕ_r is limited in practice, α is adopted instead of ϕ_r. Here α represents the ratio of the mobilised shearing resistance around the shield axis due to the rotation of cutter disc and the dynamic friction on the shield periphery. α in the simulation is about 0.3, which indicates that the dynamic friction on the shield periphery is sufficient to resist the shearing resistances generated by the cutter disc rotation. The well agreement of predicted and observed shield velocities v_s is also shown in Figure 5. The tendency of predicted v_s is similar to F_{3r} in Figure 2, since the shield velocity depends on the jack thrust.

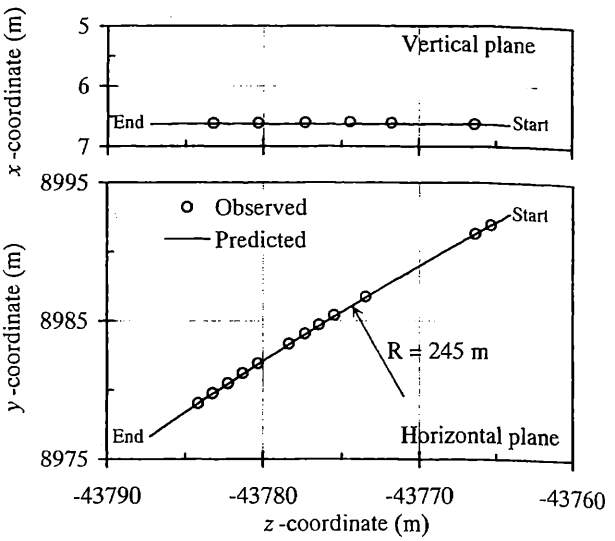

Figure 6. Predicted and observed shield traces.

The rest of above-mentioned parameters in Figure 5 show the alignment characteristics of the shield and the tunnel in the simulation, which are curvature on the horizontal and the vertical planes (κ_h and κ_v), and tilt angles from the shield traces onto the machine axis on the horizontal and the vertical planes (θ_{xT} and θ_{yT}). The inversions of κ_h and κ_v show radius of the curve on the horizontal and the vertical planes respectively. κ_h and θ_{xT} are almost slightly less than zero, this points out that curvatures of the tunnel and the shield axes are in the horizontal leftward curve. κ_h is mostly close to -0.004 which is correspondent to the horizontal curve radius of 245 m. κ_v and θ_{yT} are almost close to zero, since the shield excavates in a horizontal straight alignment. The fluctuations of κ_v and θ_{yT} are very small compared with those of κ_h and θ_{xT}. This indicates that the shield moves likely wriggle motion in the horizontal direction, where the copy cutter is used at around the left spring line of the shield.

Figure 6 shows a very good agreement between the predicted and the observed shield traces on the horizontal and the vertical planes. On the vertical plane, the predicted and observed shield traces show horizontal straight alignment, which is compatible with the planned alignment. The shield trace on the horizontal plane shows that the shield excavates in the horizontal leftward curve, which is also compatible with the planned alignment.

4 GROUND-SHIELD INTERACTION

Ground-shield interaction is discussed by considering the simulation results at the excavation step No.

122, i.e., at the distance of 150.011 m in the test site, as an example.

Here, notes that the shield periphery is unfolded as a flat plate, i.e., a vertical axis shows length of the shield and a horizontal axis represents circumference of the shield. It is also noted that the earth pressures described here are the total earth pressures. The initial normal earth pressure σ_{no} around the shield periphery at the considered location is shown in Figure 7 and distributions of the earth pressure are uniform along the length of shield because the shield excavated on the likely horizontal plane. The normal ground displacement U_n around the shield periphery caused by translation and rotation of the shield is also plotted in Figure 7. U_n is then applied to the ground reaction curve, as shown in Figure 8, to determine the normal earth pressure acting on the shield periphery σ_{ns}. σ_{ns} distribution on the shield periphery is also drawn in Figure 7. The intensity of σ_{ns} is at the area where U_n is positive. This figure also shows that σ_{ns} is in passive state for the positive U_n, whereas negative U_n generates σ_{ns} in active state.

Since the copy cutter was mostly applied in the range of 10° to 160°, U_n is changed drastically around at 10° to 160° as well as at the opposite side.

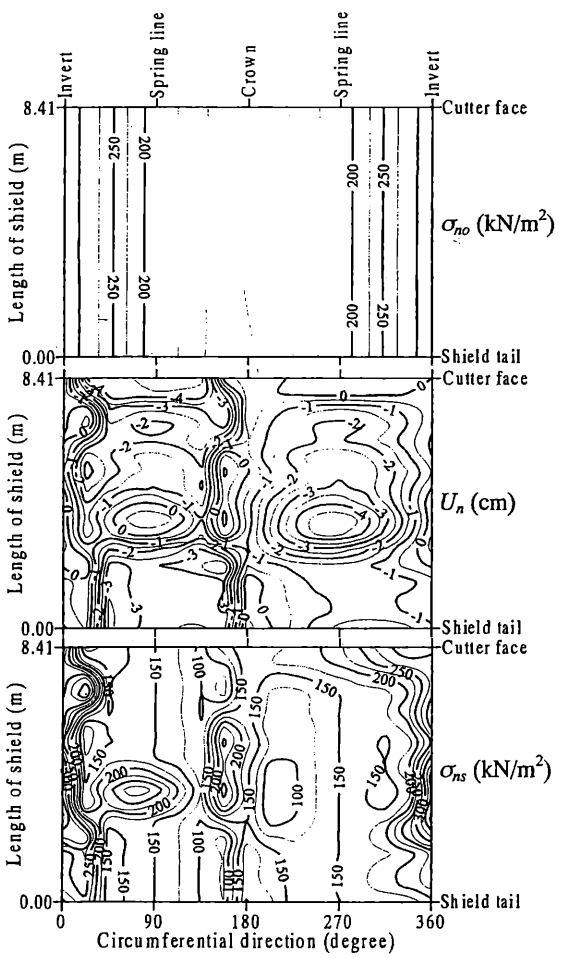

Figure 7. σ_n and U_n around shield at distance of 150.011 m.

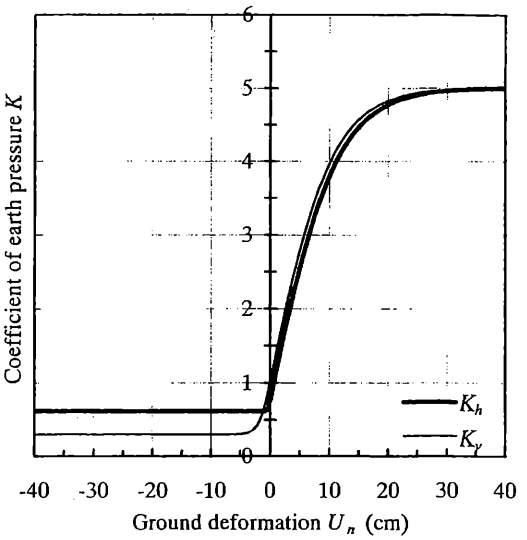

Figure 8. Ground reaction curves for medium stiff clay layer.

U_n at the left spring line around the middle length of shield becomes positive, where the shield skin plate pushes the ground, whereas at the opposite side U_n becomes negative, where the gap appears between the shield skin plate and the ground. Furthermore, U_n becomes close to zero at the shield tail around the right spring line of the shield, whereas at the opposite side U_n becomes negative. These are because the shield rotates towards the left, i.e., the shield skin plate pushes the ground on the concave side of curve at the middle length of shield and the gap between the shield and the ground at the convex side of curve at the shield tail becomes small, in order to satisfy the equilibrium condition.

U_n on the section through spring lines of the shield can be simply illustrated as shown in Figure 9. From this figure, it is clear that negative U_n, i.e., the gap between the shield skin plate and the ground, at the spring lines are mostly generated and positive U_n, i.e., the shield pushing the ground, appears only at the middle length of the shield at the left spring line.

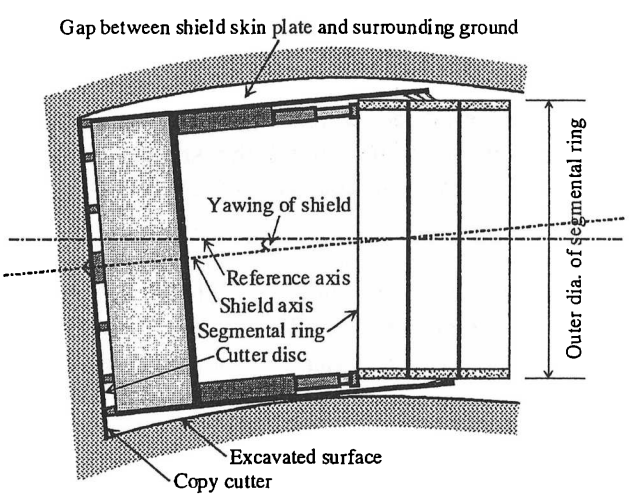

Figure 9. Illustration of gap around shield during excavation.

Table 2. Force and moment acting on shield (L=150.011 m).

Type	Force and moment components (kN, kN-m)					
	F_p	F_q	F_r	M_p	M_q	M_r
f_1	4686	0	-5	0	1945	0
f_2	-1	11	-224	53	4	240
f_3	0	0	13960	1703	-8711	0
f_4	-95	-4	-10324	-19	1539	-3848
f_5	-4590	-7	-3407	-1737	5223	3608
ΣF	0	0	0	0	0	0

This points out that use of the copy cutter mainly generates the gap between the shield skin plate and the ground and the rotation of shield causes variation of the gap around the shield.

Forces and moments acting on the shield are summarised in Table 2. Here notes that F and M are the force and the moment acting on the shield respectively, whereas the subscripts p, q and r are the directions in machine coordinate system and the subscripts number are the types of the forces as shown in Fig. 4. The force and moment components due to f_1 are almost constant, since the shield moved in a horizontal straight alignment. The force and moment components of f_3 are variation as shown in Figure 2 so as to adjust the shield position and the shield postures onto the planned tunnel alignment. The force and moment components of f_2, f_4 and f_5 are generated by changing the shield behaviour in order to satisfy the equilibrium condition as shown in Table 2.

5 CONCLUSIONS

The shield tunnelling behaviour at the curve alignment was simulated to verify performance of the shield model. As a result, the conclusions can be made as follows:

1. The model of the loads acting on the shield can simulate the shield behaviour at the curve alignment reasonably well.
2. The tunnel operational controls are factors affecting the shield behaviour and the use of copy cutter is a predominant factor affecting the shield rotation.
3. The earth pressure acting on the shield, especially on the shield periphery, which is determined from the ground displacement around the shield, influences the deviations and rotations of shield during excavation.
4. The use of copy cutter is the main factor to generate the gap between the shield periphery and the ground. Furthermore, the shield rotation is found to be the cause of the gap variation around the shield during excavation at the curve alignment.

REFERENCES

Sugimoto, M. & Sramoon, A. 2002. Theoretical model of shield behavior during excavation I: Theory. *Journal of Geotechnical and Geoenvironmental Engineering*. 128(2): 138-155.

Sramoon, A., Sugimoto, M. & Kayukawa, K. 2002. Theoretical model of shield behavior during excavation II: Application. *Journal of Geotechnical and Geoenvironmental Engineering*. 128(2): 156-165.

Takahashi, K. & Fukazawa, N. 2001. Challenge to cylindrical enlargement of shield machines and underground docking. In T. Adachi et al. (eds), *Modern Tunneling Science and Technology*: 913-918. Lisse: Swets & Zeitlinger.